N-cadherin can structurally substitute for E-cadherin during intestinal development but leads to polyp formation

Lenka Libusova[1,*], Marc P. Stemmler[1,†], Andreas Hierholzer[1], Heinz Schwarz[2] and Rolf Kemler[1]

SUMMARY

We conditionally substituted E-cadherin (E-cad; cadherin 1) with N-cadherin (N-cad; cadherin 2) during intestine development by generating mice in which an *Ncad* cDNA was knocked into the *Ecad* locus. Mutant mice were born, demonstrating that N-cad can structurally replace E-cad and establish proper organ architecture. After birth, mutant mice gradually developed a mutant phenotype in both the small and large intestine and died at ~2-3 weeks of age, probably due to malnutrition during the transition to solid food. Molecular analysis revealed an extended domain of cells from the crypt into the villus region, with nuclear localization of β-catenin (β-cat; Ctnnb1) and enhanced expression of several β-cat target genes. In addition, the BMP signaling pathway was suppressed in the intestinal epithelium of the villi, suggesting that N-cad might interfere with BMP signaling in the intestinal epithelial cell layer. Interestingly, mutant mice developed severe dysplasia and clusters of cells with neoplastic features scattered along the crypt-villus axis in the small and large intestine. Our experimental model indicates that, in the absence of E-cad, the sole expression of N-cad in an epithelial environment is sufficient to induce neoplastic transformations.

KEY WORDS: Mouse, Cadherins, Intestine, Dysplasia, Gene replacement

INTRODUCTION

Dynamic and regulated cell-cell adhesion plays a fundamental role in the development of multicellular organisms. Cadherins are key regulators of cell-cell adhesion and their expression patterns often correlate with important morphogenetic processes during development (Gumbiner, 2005; Takeichi, 1988). This is exemplified by the reciprocal expression of E-cadherin [E-cad; cadherin 1 (Cdh1)] and N-cadherin [N-cad; cadherin 2 (Cdh2)] during gastrulation, neural plate formation and eye development. E-cad is vital for trophectoderm formation during mouse preimplantation development and later its expression is largely confined to epithelial cells (Stemmler, 2008). At gastrulation, E-cad is downregulated in the emerging mesoderm, where N-cad becomes expressed. N-cad expression is restricted to neural tissues, the notochord and mesenchymal derivatives (Takeichi, 2007). Opposing roles of E-cad and N-cad are also observed during tumor formation. In tumors of epithelial origin, E-cad acts as an invasive suppressor, whereas de novo N-cad expression correlates with invasiveness, increased motility and metastatic potential of cancer cells (Hazan et al., 2004; Tomita et al., 2000).

E-cad and N-cad are the most prominent members of the cadherin family of adhesion molecules, and a large body of information about them has been collected. The two cadherins share several structural and functional features, notably the Ca^{2+}-dependent homophilic interactions of the extracellular domains and the association of the intracellular domains with catenins (Kemler, 1993). Their adhesive function can be modulated by kinases or

small GTPases, and the differential association of these cadherins with growth factor receptors suggests that they are involved in signaling pathways (Stemmler, 2008).

Recently, we addressed the interchangeability of these two proteins by substituting E-cad by N-cad using a knock-in strategy in mice (Kan et al., 2007). With this approach, N-cad was efficiently expressed in the E-cad expression domain during development and in adult tissues. Heterozygous mice co-expressing E-cad and N-cad showed normal embryonic development and were viable. However, homozygous *Ncad* knock-in embryos failed to form a functional trophectoderm, underlining the specific requirement for E-cad at this developmental stage. Interestingly, homozygous *Ncad* knock-in embryonic stem (ES) cells formed teratomas, which contained various epithelial-like structures. These results suggest that N-cad can support the formation of epithelia in the absence of E-cad (Kan et al., 2007). To further explore whether N-cad can promote epithelial integrity and function, we chose to analyze the epithelium of the mammalian intestine. The epithelium of the small intestine forms two functionally distinct compartments: invaginated crypts and finger-like protrusions termed villi. In the crypt compartment, self-renewing stem cells produce Paneth cells and rapidly dividing transit-amplifying cells. The latter migrate away from the bottom of the crypt and differentiate into the three major cell lineages of the villi (for a review, see Barker et al., 2008).

To replace E-cad with N-cad in the developing intestine, we have generated compound mice composed of an *Ncad* knock-in allele, a floxed *Ecad* allele, and a villin-Cre (*Vil-Cre*) transgene, which begins to be expressed at embryonic day (E) 10.5 in the entire intestinal epithelium (el Marjou et al., 2004). We show that N-cad can support embryonic gut development, but that these mice develop a mutant phenotype after birth.

[1]Department of Molecular Embryology, Max-Planck Institute of Immunobiology, Stuebeweg 51, D-79108 Freiburg, Germany. [2]Max-Planck Institute of Developmental Biology, Spemannstr. 35, D-72076 Tübingen, Germany.

*Present address: Charles University, Faculty of Science, Department of Cell Biology, Vinicna 7, 12844 Prague 2, Czech Republic
†Author for correspondence (stemmler@immunbio.mpg.de)

MATERIALS AND METHODS
Mouse strains
The generation of *Vil-Cre* transgenic mice, *Ecad*[+/Ncad] and *Ecad*[flox/flox] mice is described elsewhere (Boussadia et al., 2002; el Marjou et al., 2004; Kan et al., 2007). All strains were maintained on a C57BL/6 background. *Ecad*[flox/flox] females were crossed with *Ecad*[+/Ncad];*Vil-Cre* males, and the

resulting *Ecad*^{flox/Ncad};*Vil-Cre* mutants were analyzed in parallel with their *Ecad*^{flox/+};*Vil*-Cre and *Ecad*^{flox/Ncad} littermates. Experimentation with mice was according to German Animal Welfare regulations.

Histology, immunohistochemistry and BrdU labeling

Samples of the small intestine were fixed in 4% paraformaldehyde, dehydrated, paraffin-embedded and sectioned at 7 μm for both Hematoxylin and Eosin staining and the immunostaining procedure. Immunohistochemistry on paraffin sections was performed as described previously (Barker et al., 2009; Batlle et al., 2002). The following antibodies were used: anti-N-cad (1:300, BD Transduction Laboratories), anti-E-cad (1:300, BD), anti-β-cat (1:300, BD), anti-unphosphorylated β-cat (1:200, Upstate), anti-villin (1:300, S. Robine, Institut Curie, Paris), anti-chromogranin (1:50, Progen), anti-lysozyme (1:500, DakoCytomation), anti-Ascl2 (1:100, R&D), anti-cyclin D1 (1:100, Dianova) and anti-P-Smad 1, 5, 8 (1:200, Cell Signaling). For detection, the peroxidase-conjugated DAKO Envision+ System (DakoCytomation) was used.

For BrdU labeling, mice were injected intraperitoneally with 100 μg BrdU (Sigma) per gram of body weight and analyzed 2 hours later. Intestinal samples were processed as above with the addition of antigen; retrieval slides were incubated in 2 M HCl for 1 hour at 37°C and subsequently neutralized with 0.1 M borate buffer, pH 8.5. BrdU-labeled nuclei were detected with rat anti-BrdU (1:3000, Accurate). Sections were counterstained with Carazzi's Hematoxylin for 2 minutes.

Immunofluorescence labeling

Fresh samples of small intestine were embedded in OCT (Tissue-Tek), frozen and sectioned at 10 μm. Cryosections were fixed with 3% paraformaldehyde, permeabilized with 0.3% Triton X-100 and blocked in 2% BSA. Primary antibodies were used as for immunohistochemistry. Species-specific secondary antibodies conjugated with Alexa 488 and Alexa 555 (1:300) were obtained from Molecular Probes. Sections were mounted in Prolong Gold Antifade Reagent containing DAPI (Molecular Probes). Images were acquired using an LSM510 confocal microscope and Zeiss imaging software.

Transmission electron microscopy

Intestinal samples were fixed in 2% paraformaldehyde/2.5% glutaraldehyde/PBS for 5 minutes at room temperature and for 1 hour at 4°C, then postfixed with 1% osmium tetroxide in 100 mM phosphate buffer pH 7.2 for 1 hour on ice and, after rinsing with double-distilled water, were treated with 1% aqueous uranyl acetate for 1 hour at 4°C. Samples were dehydrated through a graded series of ethanol and embedded in Epon. Ultrathin sections were stained with uranyl acetate and lead citrate and viewed in a Philips CM10 electron microscope.

Isolation of intestinal epithelial cells

Rinsed small intestine was cut into small pieces, and epithelial cells were detached from the lamina propria by incubation in isolation buffer (30 mM EDTA in Mg^{2+}-free, Ca^{2+}-free Hank's balanced salt solution) and vigorous vortexing (Traber et al., 1991). Suspended cells were collected by brief centrifugation, washed with PBS and immediately used for RNA or protein extraction.

Western blot analysis

Protein lysates were prepared from isolated intestinal epithelial cells using a 1:1 mixture of protein extraction buffer (20 mM Tris pH 7.8, 2 mM EDTA, 200 mM NaCl) and PhosphoSafe Extraction Buffer (Merck Chemicals), supplemented with 0.5% Triton X-100 and protease inhibitor cocktail (Roche). Equal amounts of protein were separated by SDS-PAGE and transferred to a nitrocellulose membrane. Membranes were probed with the following antibodies: anti-E-cad, anti-N-cad (1:2000), anti-Smad7 (1:1500, R&D), mouse anti-actin (1:3000, Biozol) and rabbit anti-P-Smad 1, 5, 8 (1:1000, Cell Signaling). HRP-conjugated secondary antibodies (Jackson ImmunoResearch) and ECL Plus detection reagent (GE Healthcare) were used for detection.

RNA extraction and quantitative (q) RT-PCR

Total RNA was prepared from isolated epithelial cells (see above) using the RNeasy Mini Kit (Qiagen). DNaseI-treated RNA was converted to cDNA using the Superscript III First Strand Synthesis Kit (Invitrogen) primed by random hexamers. qPCR was performed using the ABsolute QPCR ROX Mix (ABgene) in combination with the mouse Universal Probe Library (Roche) according to the manufacturer's instructions. Results were obtained from at least two experiments performed in triplicate, and error bars indicate s.e.m. Primer sequences for each gene are provided in Table S1 in the supplementary material.

RESULTS

Analysis of the substitution of E-cad with N-cad

In *Ecad*^{flox/Ncad};*Vil-Cre* mutant mice, the vast majority of the gut epithelium lacked E-cad during embryonic development (E17.5; see Fig. S1 in the supplementary material) as well as postnatally [postnatal day (P) 16, Fig. 1A]. Thus, E-cad was efficiently deleted during development and replaced by N-cad. Importantly, the exogenous N-cad exhibited a basolateral plasma membrane localization in the epithelium of the villi, indicating an intact apical-basal cell polarity required for tissue integrity (see Fig. S2A in the supplementary material). Small patches of E-cad-positive epithelial cells were observed sporadically in the mutant intestine (Fig. 1A), which was likely to be due to a small number of crypt stem cells escaping Cre-mediated recombination. In these epithelial cells, E-cad and N-cad were colocalized on the membrane (see Fig. S2B in the supplementary material), similar to what has been observed in *Ecad*^{+/Ncad} mice (Kan et al., 2007). Western blot analysis of isolated epithelial cells from control and mutant intestines showed some residual E-cad protein in the mutants (see Fig. S2C in the supplementary material), consistent with the results described above (Fig. 1A).

Staining for β-catenin (β-cat; Ctnnb1 – Mouse Genome Informatics), a key component of the adherens junction, revealed membrane localization in mutant and control epithelial cells along the entire crypt-villus axis (Fig. 1B). Mutant and control intestines were also stained for p120 (Ctnnd1 – Mouse Genome Informatics) and junction plakoglobin. Both proteins displayed clear membrane staining along the crypt-villus axis, although p120 was additionally distributed in the cytoplasm of mutant epithelial cells (see Fig. S1D in the supplementary material). Analysis of cell polarity by staining for Na^+/K^+-ATPase gave comparable results in control and mutant epithelial cells (not shown). Cellular architecture and integrity were further analyzed by transmission electron microscopy, without any indication of alterations in the mutant epithelial cells (Fig. 1C). In mutants, both tight and adherens junctions were fully formed, similar to control small intestine samples (Fig. 1C). Likewise, the morphology of the mutant cells, including the brush border region, did not show any signs of aberration. From these results, we conclude that N-cad can structurally substitute for E-cad in the intestinal epithelial cell layer.

Phenotype of *Ecad*^{flox/Ncad};*Vil-Cre* mice

After birth, the gut of mutant and control mice was examined morphologically and histologically at P5, P8 and P14-17. With age, mutant mice gradually developed an aberrant phenotype in their intestinal tracts. The mutant mice became less active and were small, reaching only 60% of the body weight of their control littermates (see Fig. S5A in the supplementary material). The life expectancy of the mutants was poor and they were unable to switch to a diet of solid food and died around weaning (~P19). The intestines of the mutants were much larger than normal in diameter,
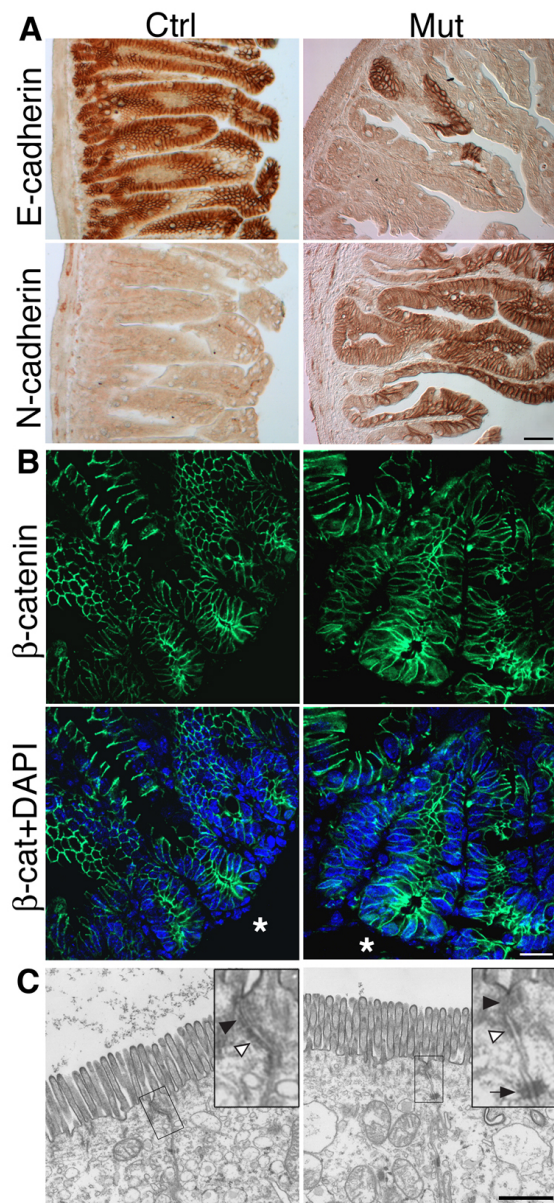
Fig. 1. N-cad replaces E-cad at the basolateral membrane of the Ecad^{flox/Ncad};Vil-Cre mutant intestinal epithelium.
(**A**) Immunohistochemical staining on paraffin sections of P16 mouse intestine showing E-cad at the epithelial plasma membrane of control animals (Ctrl). In mutants (Mut), E-cad is replaced by N-cad. (**B**) β-cat binds to both E-cad and N-cad at the plasma membrane (BD antibody). Higher levels of β-cat are detected in both the nuclei and the cytoplasm of mutant intestinal epithelium. Asterisk indicates submucosa. (**C**) Electron micrograph of intestinal epithelium of P0 mutant and control animals. No changes in the ultrastructure of tight junctions (black arrowheads), adherens junctions (white arrowheads) or desmosomes (arrow) were detected in the mutant epithelium. Scale bars: 50 μm in A; 40 μm in B; 1 μm in C.

but the caecum was disproportionately small (data not shown). The overall appearance of the intestines was rather pale, with aqueous content in the lumen. In histological sections of the small intestine, mutant villi were significantly longer than normal and often misshapen and branched (Fig. 2A).

Using differential staining for goblet cells [periodic acid-Schiff staining (PAS)], enteroendocrine cells (Grimelius stain) or connective tissue (van Gieson stain), differentiated derivatives of the intestinal cell lineages were detected in the mutants (see Fig. S3 in the supplementary material; data not shown). In agreement with the histological differential staining results, immunohistochemical analysis showed that absorptive cells are present in both the mutant and control intestinal samples, with anti-villin (villin 1 – Mouse Genome Informatics) staining at the brush borders of epithelia throughout the entire villus region (see Fig. S3 in the supplementary material). A considerable reduction was detected in the other three cell types of the intestinal epithelium. Lysozyme-positive Paneth cells, chromogranin-positive enteroendocrine cells, and goblet cells detected by PAS staining were present in much lower numbers in the mutant than control (see Fig. S3 in the supplementary material).

Blood samples of mutant and control mice were taken at P14. As a major difference, we found an increase in α-amylase and a reduction in cholinesterase levels in the mutant (not shown). The analysis demonstrated that the reduction in differentiated cell types required for proper food digestion and nutrient uptake in the mutant intestine presumably leads to chronic malnutrition and lethality, as suggested by decreased cholinesterase in the blood serum. Notably, clusters of cells with severe dysplastic features and polyps were observed in the intestines of mutant mice at ~2 weeks of age (Fig. 2A). These neoplastic lesion structures were characterized by unpolarized, multilayered epithelial cells with dysplastic and enlarged polymorphic nuclei (Fig. 2A, arrowheads), a high degree of proliferation (Fig. 2B) and altered expression of CD44 and annexin A1, which are indicators of adenomas (Gaspar et al., 2008) (data not shown). Similarly, polyps were found in the colon of mutant mice (see Fig. S4 in the supplementary material). The frequency of these polyps and their severity varied markedly between individuals. In some severe cases there were 4-8 polyps per centimeter of intestine, but in general they occurred to a much lesser extent than, for example, in mice carrying mutations that lead to the stabilization of β-cat (Harada et al., 1999; Su et al., 1992).

The proliferative status of the epithelium in the small intestine was examined by 5-bromo-2-deoxyuridine (BrdU) incorporation (Fig. 2C). Mice were given a 2-hour pulse of BrdU, and the labeling rates were compared in corresponding parts of the mutant and control epithelium. The percentage of BrdU-positive cells in the intestine of the mutants was more than twice that of the control animals (see Fig. S5B in the supplementary material). A similar increase in proliferating Pcna-positive cells was detected in less dysplastic regions of the mutant intestine (see Fig. S5C in the supplementary material). This indicates that substituting E-cad with N-cad results in increased cell proliferation, which in turn leads to the hyperplastic changes observed throughout the entire intestinal tract.

Enhanced β-catenin signaling activity in *Ncad* knock-in intestinal epithelial cells

Hyperproliferation of intestinal epithelial cells is often connected with an aberrant activation of β-cat signaling. Several studies have shown that β-cat, in complex with Tcf4, controls the expression of *c-Myc*, cyclin D1 and other target genes, which in turn inhibit differentiation and promote cell proliferation (Tetsu and McCormick, 1999; van de Wetering et al., 2002). We analyzed the subcellular distribution of the specific β-cat form that plays a role in Wnt signaling (active β-cat, unphosphorylated at Ser37 and
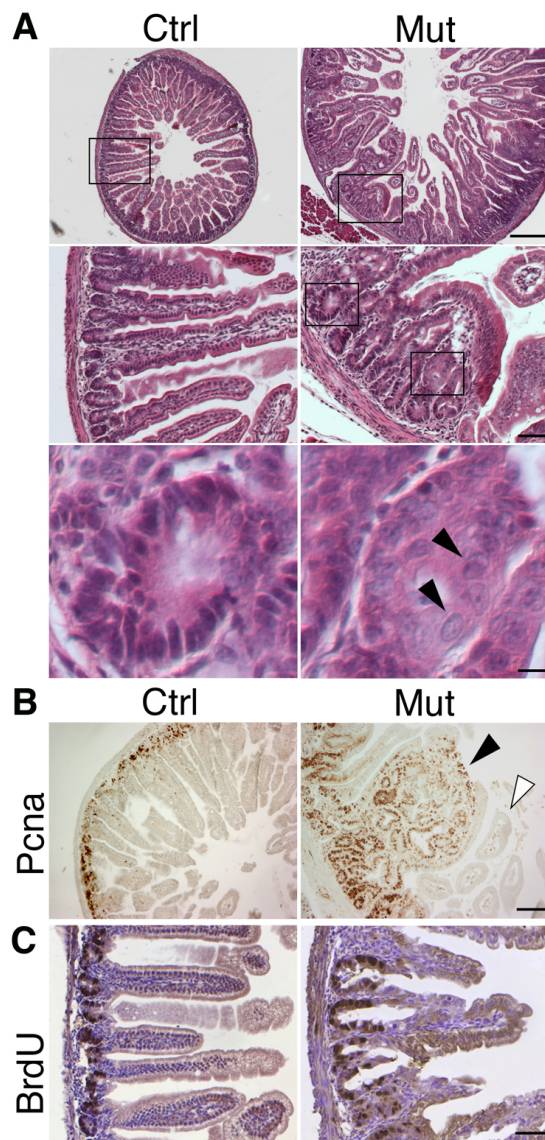
Fig. 2. Mice expressing N-cad in the absence of E-cad in the gut epithelium suffer from morphological changes in the small and large intestine and form polyps. (**A**) Hematoxylin and Eosin staining of mouse small intestine sections reveals morphological changes in the size of the lumen, disorganization of the crypt and villus compartment, and the appearance of polyps. Neoplastic lesions with enlarged polymorphic nuclei (bottom right, arrowheads) and a region of control intestine (bottom left) are shown at higher magnification. (**B**) Immunohistochemistry of Pcna reveals increased cell proliferation in adenomatous structures (black arrowhead) in comparison to villi (white arrowhead) and controls. (**C**) Hyperproliferation of epithelial cells in the crypts is evident by an increase in BrdU-labeled cells. Scale bars: in A, 250 μm (top), 50 μm (middle), 10 μm (bottom); 25 μm in B; 50 μm in C.

Fig. 3. Wnt signaling is increased in the mutant intestine due to relocalization of β-cat. (**A**) Immunohistochemical staining of β-cat and the stem cell marker Ascl2. Nuclei of mutant epithelium contain high amounts of the active (non-phosphorylated, Upstate antibody) form of β-cat (top right), which was displaced from the plasma membrane, in contrast to in control mice (top left). In the control intestine, Ascl2-positive cells are restricted to the crypt region (bottom left), whereas in the mutant intestine the progenitor cell compartment is expanded into the villus compartment (bottom right). Scale bar: 50 μm. (**B**) qRT-PCR expression analysis of selected Wnt target genes showing elevated transcript levels in mutant (black) versus control (gray) epithelium.

Thr41) (van Noort et al., 2002). In control littermates, nuclear β-cat accumulated only in cells at the bottom of the crypts (Fig. 3A). Active Wnt signaling in this region is known to regulate the pool of progenitor cells (Pinto et al., 2003). Remarkably, in the epithelium of the *Ncad* knock-in mutant mice, β-cat was present prominently in the nuclei of crypt cells and cells of the villu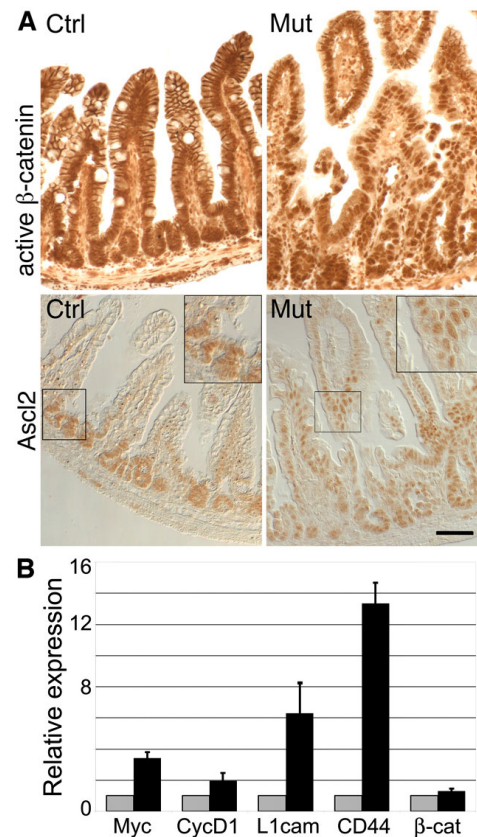s region, even outside of dysplastic regions (Fig. 3A, top). Distinct membrane localization of unphosphorylated β-cat in mutant intestines was only observed in cells at the tips of the villi (Fig. 3A). These results suggest that the substitution of E-cad with N-cad induces ectopic activation of β-cat signaling outside the bottom of the crypts. Additional support for this hypothesis was provided by the striking increase in expression of the Wnt/β-cat target gene cyclin D1, which showed an expanded expression domain in the crypts and the bottom of the villi in the intestine of mutant mice compared with that of control animals (see Fig. S5C in the supplementary material, bottom). Concomitantly, the spread in Wnt/β-cat signaling into the villus region led to an enlargement of the progenitor cell pool, as indicated by increased staining of nuclei of mutant villus epithelium for the stem cell marker Ascl2 (Fig. 3A, bottom right) (van der Flier et al., 2009). In control samples, Ascl2 was restricted to the crypt epithelium (Fig. 3A, bottom left).

To verify that the accumulation of nuclear β-cat in the mutant intestine is associated with the induction of other known Wnt targets, we performed qRT-PCR for *c-Myc*, *L1cam* and *Cd44*,

which are involved in cell proliferation and tumorigenesis in the gut (Boo et al., 2007; Pinto et al., 2003; Zeilstra et al., 2008). All three genes were significantly upregulated in intestinal epithelial cells isolated from mutants as compared with control epithelium: *Cd44* was upregulated more than 10-fold (Fig. 3B). CD44 is clearly associated with the proliferative compartment of the gut as well as with dysplastic lesions (van de Wetering et al., 2002). Although a striking difference in immunostaining was detected for cyclin D1, only a moderate induction of mRNA was found in the mutant epithelium. Levels of mRNA for β-cat were comparable in control and mutant epithelia (Fig. 3B).

Repressed BMP signaling in the *Ncad* knock-in intestinal epithelium

There is accumulating evidence for complex cross-talk between multiple pathways in the intestinal epithelium. Besides Wnt signaling, the BMP pathway plays a fundamental role in controlling the balance between cell regeneration and differentiation along the crypt-villus axis. The BMP pathway appears to counteract Wnt signaling by repressing stem cell renewal, crypt fission and polyp formation (Haramis et al., 2004; He et al., 2004; Tian et al., 2005). Accordingly, we investigated the BMP signaling pathway in the *Ncad* knock-in mutant epithelium.

Active BMP signaling is reflected in the nuclear localization of intracellular transducers, specifically phosphorylated Smads 1, 5 and 8 (P-Smad 1, 5, 8). In the intestinal epithelium of control animals, P-Smad 1, 5, 8 localized to the nuclei of epithelial cells in the villus region, but the crypt region was mostly devoid of P-Smad 1, 5, 8 (Fig. 4A, left). By contrast, P-Smad 1, 5, 8 expression was rather weak and irregular in mutant intestines, with only occasionally distinct nuclear localization (Fig. 4A, right). Consistently, less P-Smad 1, 5, 8 was found in the protein lysates of mutant epithelial cells, as detected by western blot (Fig. 4B), which indicates that BMP signaling is reduced throughout the entire epithelium of the mutant intestine. To test whether the decrease in phosphorylated Smads is accompanied by an alteration in BMP target gene expression, we examined the transcript levels of several established BMP targets, including *Id2*, *Id3* and the inhibitory Smads *Smad6* and *Smad7*. Expression of these target genes was strongly impaired in mutants relative to the controls (Fig. 4C). Consistent with this, Smad7 protein was decreased in the epithelium isolated from mutant mice (Fig. 4B). This indicates that BMP signaling is dysregulated in the mutant intestine.

Enhanced activation of the Wnt pathway precedes repression of the BMP signaling cascade in the *Ncad* knock-in intestine

All experiments performed so far concerned a fully developed mutant phenotype (P14-17). It was of interest to explore potential alterations in the Wnt and BMP pathways during late embryogenesis and in neonatal mice, in which the intestine starts to function as a digestive organ, and to see whether changes appear simultaneously or whether one pathway is affected first. We examined intestinal sections of mutant and control animals at different stages for dephosphorylated β-cat and for P-Smad 1, 5, 8 as indicators of Wnt and BMP signaling activity, respectively. During development, for example at E17.5, there were no apparent differences in the signal intensities of β-cat or P-Smad 1, 5, 8 between mutant and control intestinal sections (data not shown). By contrast, newborn (P0) pups revealed a distinct accumulation of β-cat in the nuclei of many mutant epithelial cells, whereas it
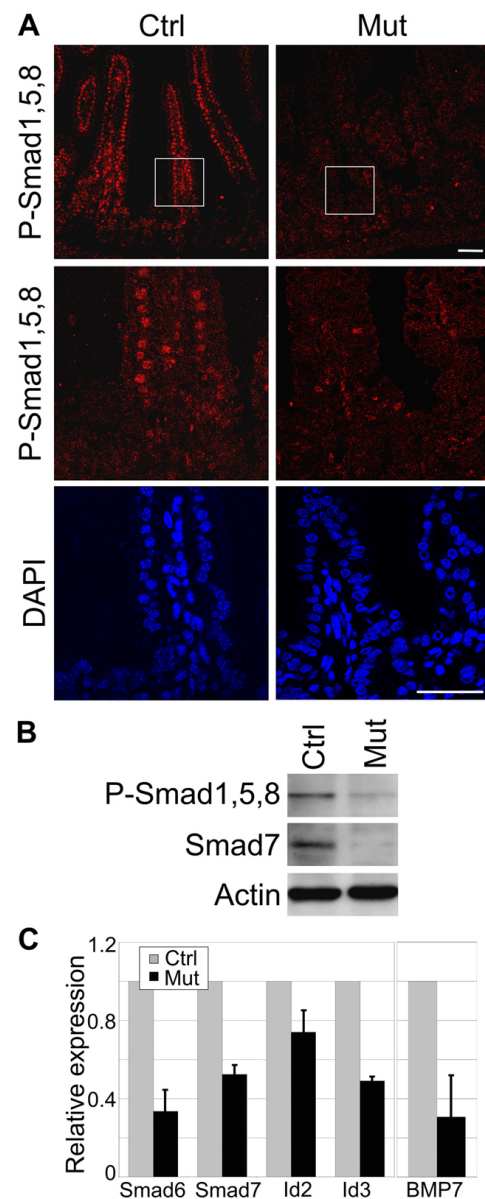

Fig. 4. Loss of BMP signaling in the mutant epithelium. (**A**) Active BMP signaling is detected by immunofluorescence staining for activated (phosphorylated, P) forms of the downstream transducers Smad 1, 5, 8 in intestines at P16. Smad 1, 5, 8 is present in the villus region but absent from crypts in the control gut (Ctrl). In mutants (Mut), P-Smad 1, 5, 8 is largely undetectable in all regions. The boxed regions are shown at higher magnification in the middle and bottom (nuclei, DAPI) rows. Scale bar: 50 μm. (**B**) Western blot of control and mutant epithelium cell lysates confirms the reduced levels of P-Smad 1, 5, 8 as well as of the downstream target Smad7 in the mutant epithelium. (**C**) qRT-PCR expression analysis shows an overall reduction of *Bmp7*, which is the only ligand expressed in the intestinal epithelium, and of BMP target genes.

was restricted to the bottom of the crypt in the control epithelium (Fig. 5A). Additionally, the amount of membrane-bound β-cat was already reduced in the epithelium of mutants when compared with that of controls (Fig. 5A). By contrast, P-Smad 1, 5, 8 exhibited a comparable staining pattern in the control and mutant intestine (Fig. 5B). In mutant and control samples, the nuclear P-Smad 1,
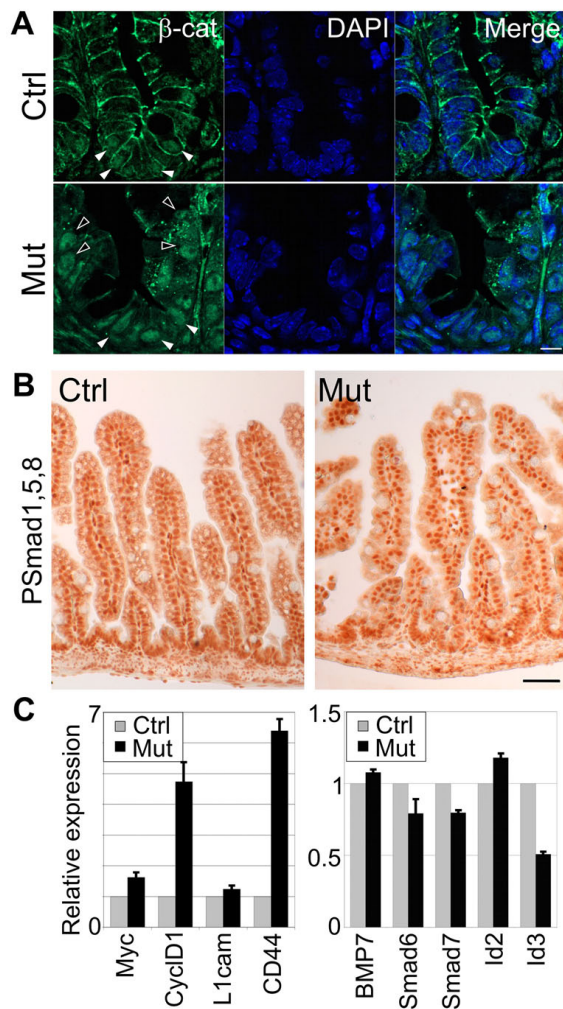
Fig. 5. Changes in Wnt signaling are first detectable in the immature intestine of newborn mice and precede changes in BMP signaling. (**A**) The area of Wnt signaling is expanded in the intestine of mutant P0 mice as shown by translocation of non-phosphorylated β-cat (green) from the membrane to the nucleus (DAPI, blue). β-cat-positive nuclei at the bottom of the crypt are indicated by white arrowheads and those outside of that region by black arrowheads. Scale bar: 10 μm. (**B**) No alteration in BMP signaling is detected in mutant versus control intestines, as indicated by an identical distribution of P-Smad 1, 5, 8. Scale bar: 50 μm. (**C**) qRT-PCR analysis of Wnt (left) and BMP (right) target genes confirms the early onset of enhanced Wnt signaling in the mutant intestinal epithelial cells.

5, 8 signal was strong along the villus and also in the crypt region because the BMP pathway displays high activity in the developing immature intestine (He et al., 2004). These results suggest that signaling through β-cat is already altered in P0 mutant intestines, whereas BMP signaling is still normal.

To analyze this possibility in more detail, we compared target gene expression of both pathways in control and mutant intestinal epithelia by qRT-PCR. The enhanced nuclear function of β-cat in the newborn mutant intestine was further confirmed by detecting the dysregulation of Wnt target genes. Except for *L1cam*, all other target genes were strongly upregulated (Fig. 5C). In contrast to these findings, but in agreement with P-Smad 1, 5, 8 staining, BMP target genes were not substantially altered (Fig. 5C).

These results indicate that alterations in signaling pathways appear postnatally, initiated by an increased nuclear accumulation of β-cat in an enlarged crypt region. Since BMPs, P-Smads and BMP target genes are unaffected at P0, we conclude that alterations in the Wnt pathway precede changes in BMP signaling in the mutant intestine. This observation raised the possibility that the enhanced expression of β-cat target genes might influence the BMP signaling pathway. Hence, the expression of some candidate genes that are known to either bridge both pathways or modulate activity of one of these pathways was compared by qRT-PCR analysis in control and mutant intestinal epithelial cells at P0 and P14. We compared levels of R-spondin 1 (*Rspo1* – Mouse Genome Informatics), which activates canonical Wnt signaling and induces proliferation in the intestinal epithelium upon overexpression (Kim et al., 2005; Kim et al., 2008); *Bambi*, which is a canonical Wnt target gene that promotes β-cat nuclear translocation, the expression of Wnt target genes and antagonizes BMP receptor signaling (Lin et al., 2008; Sekiya et al., 2004); gremlin 2, a secreted antagonist of BMP that is upregulated by Wnt3a (Klapholz-Brown et al., 2007); and *Pten* and 14-3-3ζ (*Ywhaz* – Mouse Genome Informatics) which have recently been reported to bridge BMP and Wnt signaling pathways in the intestine (He et al., 2004; Tian et al., 2004; Tian et al., 2005). In addition, we analyzed BMP receptors and calponins. Calponin 2 inhibits BMP signaling by sequestering Smad 1, 5, 8 to the cytoskeleton (Haag and Aigner, 2007). The results of the qRT-PCR analysis are depicted in Fig. S6 in the supplementary material. The expression of most of the genes examined was altered in the mutant epithelium at P0 and P14; some genes were affected only moderately, whereas others might be of significance for phenotype development. In particular, the expression of R-spondin 1 was strongly induced at P0 but unchanged at P14, comparing mutant with control intestine. No differences in the expression of calponin 2 and 3 were found at P0, but calponin 2 expression was 3.8-fold upregulated in the mutant epithelium as compared with the control at P14. Interestingly, the expression of BMP receptors was already reduced at P0, although BMP ligands and target genes were not yet affected at this stage (Fig. 5C). *Pten* was downregulated at P0 and P14 and 14-3-3ζ was unchanged at P0, but slightly upregulated at P14 in mutant versus control samples. The analysis shows that substituting E-cad with N-cad in the intestinal epithelium affects the expression of several components of the Wnt and BMP pathways.

DISCUSSION

E-cad is expressed by all epithelial cells along the crypt-villus axis and is indispensable for proper homeostasis and integrity of the intestinal epithelial cell layer. For correct organ function, tight regulation of the gene and its protein synthesis act in concert to control E-cad abundance at the cell surface. Forced overexpression of E-cad in the gut slows down cell migration along the crypt-villus axis and increases the apoptotic rate of epithelial cells (Hermiston et al., 1996). Expression of a dominant-negative N-cad that lacks the extracellular domain leads to the disruption of cell-cell and cell-substrate contacts and loss of cell polarity (Hermiston and Gordon, 1995). Similarly, loss of E-cad from cell-cell contacts induces anoikis in enterocytes (Fouquet et al., 2004).

Here, we used a genetic approach to replace E-cad with N-cad in the intestinal epithelium. We show that N-cad can support embryonic gut development, but mutant mice gradually develop a moribund phenotype after birth and die at ~2-3 weeks of age. Their death coincides with the nutritional switch from maternal milk to solid food. Thus, these mutant mice might represent an interesting model with which to study the physiology of the digestive tract.

Although the overall organ architecture appeared normal, the intestine of the mutant mice develops a number of changes. These morphological changes correlate with increased cell proliferation, which is extended from the crypt into the villus region.

Interestingly, mutant intestines frequently contain cell clusters with neoplastic features and small polyps scattered along the crypt-villus axis in both the small and large intestines. This is remarkable in several aspects. During the progression of many human gastrointestinal tumors, E-cad is gradually lost at the invasive front, accompanied by a de novo expression of N-cad (the cadherin switch) (Wheelock et al., 2008). This phenomenon, which appears rather late during the multi-step process of tumorigenesis, is connected to the transition from a benign adenoma to an invasive carcinoma and correlates with poor prognosis (Yilmaz and Christofori, 2009). However, the role of the de novo N-cad expression in invasive tumor cells is at present incompletely understood. Our experimental model suggests that, in the absence of E-cad, the sole expression of N-cad in an epithelial cell environment is sufficient to induce hyperplasias. Although morphological changes in the mutant epithelium are comparable to the initial steps of tumorigenesis, a comprehensive analysis needs to be performed in future experiments to identify whether these structures share features with adenoma, hamartoma or carcinoma, using an inducible *Vil-Cre* transgenic line (*Vil-Cre-ER*[T2]).

The most striking result of the molecular analysis of the mutant intestines is the extended nuclear localization of β-cat. In the normal intestine, the canonical Wnt signaling pathway is a key player in the proliferative compartment of the crypts and maintains homeostasis in the epithelium (Pinto and Clevers, 2005). Depletion of β-cat results in a loss of progenitor cells and crypt structures and induces intestinal stem cells to terminally differentiate (Fevr et al., 2007). Accumulating evidence in genetic mouse models, as well as in human cancer, underlines that aberrant activation of the Wnt pathway and nuclear localization of β-cat lead to hyperproliferation, malformation and adenomatous polyp formation (Harada et al., 1999; Kim et al., 2005). In the mutant intestine, we observe nuclear localization of β-cat extending from the crypt into the villus region. This localization results in enhanced expression of β-cat target genes, notably *Cd44*, *L1cam*, cyclin D1 and *c-Myc*, which are all associated with neoplastic transformation in human colon cancer (Augenlicht et al., 1997; Dalerba et al., 2007; Gavert et al., 2005; Mermelshtein et al., 2005). The increase in the nuclear function of β-cat is very likely to be a major contributor to the development of the mutant phenotype. A similar phenotype, which is also caused by an enhanced nuclear function of β-cat, has been described with the conditional inactivation of Apc (Andreu et al., 2005). In that study, the ablation of Apc led to the stabilization of β-cat, whereas in our work the nuclear localization of β-cat is the result of an E-cad to N-cad switch in an epithelial cell. It is possible that the prominent nuclear localization of β-cat in the mutant intestine is due to a reduced binding of β-cat to N-cad as compared with E-cad, which could lead to a slight increase in the cytoplasmic pool of β-cat (Fagotto et al., 1996; Orsulic et al., 1999). Importantly, the increase in nuclear β-cat occurs at the bottom of the crypts in cells that are already poised to receive and transduce active Wnt/β-cat signaling. The destruction complex for β-cat is inhibited and, together with the possibly reduced ability of N-cad to complex β-cat, could in turn lead to an enlarged proliferation zone from the crypts into the villi. Alternatively, the high expression of R-spondin 1 that is already observed at P0 might also be responsible for the extended nuclear localization of β-cat.

Although the described scenario is feasible, other molecular explanations must be considered. Differences in the adhesive force of E-cad and N-cad might influence tissue homeostasis and integrity, with impact on the underlying lamina propria and submucosa. This would in turn lead to structural changes as secondary effects of decreased cell adhesion. It cannot be excluded that phenotypic changes in the mutant arise from altered protein-protein interaction. For example, both E-cad and N-cad form complexes with tyrosine kinase receptors (RTKs), which can modulate RTK-mediated signal transduction. Associations of E-cad with the epidermal growth factor receptor (Egfr) and N-cad with the fibroblast growth factor receptor (Fgfr) influence cell-cell adhesion and cell migration (Fedor-Chaiken et al., 2003; Suyama et al., 2002). Intracellular domains of E-cad and N-cad complex not only with β-cat, but also with α-catenin and p120, which regulate cell adhesion and proliferation as well (Liu et al., 2009; Scott and Yap, 2006). Staining of the mutant epithelium for p120 showed that it was partially displaced from the plasma membrane (see Fig. S2D in the supplementary material), which is in agreement with the finding that E-cad and N-cad preferentially bind to different p120 isoforms (Seidel et al., 2004). In addition, components of several other pathways, including Rho GTPases, non-receptor tyrosine kinases and several actin-binding proteins, modulate the assembly of cadherin-associated actin filaments (Abe and Takeichi, 2008; Wildenberg et al., 2006). Although a clear basolateral localization of N-cad is observed in mutant epithelium, similar to E-cad in control epithelium, the cyto-cortical interactions of N-cad may differ from those of E-cad. It will be of interest to perform similar experiments to those described here with chimeric molecules between E-cad and N-cad to elucidate whether the cytoplasmic domain of N-cad is involved in the development of the mutant phenotype.

The observed phenotype, including the formation of polyps, can be predominantly attributed to an enhanced nuclear function of β-cat, consistent with data from mice and humans (Augenlicht et al., 1997; Dalerba et al., 2007; Gavert et al., 2005; Harada et al., 1999; Mermelshtein et al., 2005; Su et al., 1992). In addition, it is possible that other pathways are dysregulated and contribute to the phenotype. The phenotype of our mouse mutants results in death 2 to 3 weeks after birth. In mouse models in which cytosolic levels of β-cat are increased, polyps form rapidly and in large numbers, but mice survive ~3 months (Harada et al., 1999; Oshima et al., 1995). Strikingly, we observe a decrease in, and a less pronounced nuclear localization of, P-Smad 1, 5, 8 during the first 2 weeks after birth. Interestingly, P-Smad 1, 5, 8 is mislocalized in the villi, whereas nuclear β-cat and ectopic target gene activation are extended into the enlarged crypt regions and to the tip of the villi.

The BMP pathway plays an important role in maintaining tissue homeostasis in the intestine (Haramis et al., 2004; He et al., 2004; Tian et al., 2005). Bmp2 and Bmp4 are produced by mesenchymal cells in the lamina propria, which is unlikely to be affected by our gene replacement in the epithelial cell layer, but ligands are also expressed within the epithelial sheet (Bmp7). Moreover, we observed a reduction in several BMP signaling components in mutant epithelial cells, notably Bmp7, BMP receptors 1A, 1B and 2 (see Fig. S6 in the supplementary material), Id genes and inhibitory Smad6 and Smad7 (Fig. 4C; see Fig. S5C in the supplementary material). Many of these components have been associated with human gastrointestinal pathologies when misexpressed (Waite and Eng, 2003). Thus, the observed alterations in BMP signaling might play an additional role in the pathophysiology of the intestinal tract of our mutant mice. It is tempting to speculate that N-cad in the villus region of the

epithelial cell layer is directly involved in suppressing BMP signaling by interfering with BMP receptor function. However, identification of the mechanism through which N-cad enhances Wnt and suppresses BMP signaling on a molecular level requires further analyses that focus on a biochemical comparison between wild-type and mutant intestinal epithelial cells in culture.

Competing interests statement
The authors declare no competing financial interests.

Supplementary material
Supplementary material for this article is available at
http://dev.biologists.org/lookup/suppl/doi:10.1242/dev.048488/-/DC1

References
Abe, K. and Takeichi, M. (2008). EPLIN mediates linkage of the cadherin catenin complex to F-actin and stabilizes the circumferential actin belt. *Proc. Natl. Acad. Sci. USA* **105**, 13-19.

Andreu, P., Colnot, S., Godard, C., Gad, S., Chafey, P., Niwa-Kawakita, M., Laurent-Puig, P., Kahn, A., Robine, S., Perret, C. et al. (2005). Crypt-restricted proliferation and commitment to the Paneth cell lineage following Apc loss in the mouse intestine. *Development* **132**, 1443-1451.

Augenlicht, L. H., Wadler, S., Corner, G., Richards, C., Ryan, L., Multani, A. S., Pathak, S., Benson, A., Haller, D. and Heerdt, B. G. (1997). Low-level c-myc amplification in human colonic carcinoma cell lines and tumors: a frequent, p53-independent mutation associated with improved outcome in a randomized multi-institutional trial. *Cancer Res.* **57**, 1769-1775.

Barker, N., van de Wetering, M. and Clevers, H. (2008). The intestinal stem cell. *Genes Dev.* **22**, 1856-1864.

Barker, N., Ridgway, R. A., van Es, J. H., van de Wetering, M., Begthel, H., van den Born, M., Danenberg, E., Clarke, A. R., Sansom, O. J. and Clevers, H. (2009). Crypt stem cells as the cells-of-origin of intestinal cancer. *Nature* **457**, 608-611.

Batlle, E., Henderson, J. T., Beghtel, H., van den Born, M. M., Sancho, E., Huls, G., Meeldijk, J., Robertson, J., van de Wetering, M., Pawson, T. et al. (2002). Beta-catenin and TCF mediate cell positioning in the intestinal epithelium by controlling the expression of EphB/ephrinB. *Cell* **111**, 251-263.

Boo, Y. J., Park, J. M., Kim, J., Chae, Y. S., Min, B. W., Um, J. W. and Moon, H. Y. (2007). L1 expression as a marker for poor prognosis, tumor progression, and short survival in patients with colorectal cancer. *Ann. Surg. Oncol.* **14**, 1703-1711.

Boussadia, O., Kutsch, S., Hierholzer, A., Delmas, V. and Kemler, R. (2002). E-cadherin is a survival factor for the lactating mouse mammary gland. *Mech. Dev.* **115**, 53-62.

Dalerba, P., Dylla, S. J., Park, I. K., Liu, R., Wang, X., Cho, R. W., Hoey, T., Gurney, A., Huang, E. H., Simeone, D. M. et al. (2007). Phenotypic characterization of human colorectal cancer stem cells. *Proc. Natl. Acad. Sci. USA* **104**, 10158-10163.

el Marjou, F., Janssen, K. P., Chang, B. H., Li, M., Hindie, V., Chan, L., Louvard, D., Chambon, P., Metzger, D. and Robine, S. (2004). Tissue-specific and inducible Cre-mediated recombination in the gut epithelium. *Genesis* **39**, 186-193.

Fagotto, F., Funayama, N., Gluck, U. and Gumbiner, B. M. (1996). Binding to cadherins antagonizes the signaling activity of beta-catenin during axis formation in Xenopus. *J. Cell Biol.* **132**, 1105-1114.

Fedor-Chaiken, M., Hein, P. W., Stewart, J. C., Brackenbury, R. and Kinch, M. S. (2003). E-cadherin binding modulates EGF receptor activation. *Cell Commun. Adhes.* **10**, 105-118.

Fevr, T., Robine, S., Louvard, D. and Huelsken, J. (2007). Wnt/beta-catenin is essential for intestinal homeostasis and maintenance of intestinal stem cells. *Mol. Cell. Biol.* **27**, 7551-7669.

Fouquet, S., Lugo-Martinez, V. H., Faussat, A. M., Renaud, F., Cardot, P., Chambaz, J., Pincon-Raymond, M. and Thenet, S. (2004). Early loss of E-cadherin from cell-cell contacts is involved in the onset of Anoikis in enterocytes. *J. Biol. Chem.* **279**, 43061-43069.

Gaspar, C., Cardoso, J., Franken, P., Molenaar, L., Morreau, H., Moslein, G., Sampson, J., Boer, J. M., de Menezes, R. X. and Fodde, R. (2008). Cross-species comparison of human and mouse intestinal polyps reveals conserved mechanisms in adenomatous polyposis coli (APC)-driven tumorigenesis. *Am. J. Pathol.* **172**, 1363-1380.

Gavert, N., Conacci-Sorrell, M., Gast, D., Schneider, A., Altevogt, P., Brabletz, T. and Ben-Ze'ev, A. (2005). L1, a novel target of beta-catenin signaling, transforms cells and is expressed at the invasive front of colon cancers. *J. Cell Biol.* **168**, 633-642.

Gumbiner, B. M. (2005). Regulation of cadherin-mediated adhesion in morphogenesis. *Nat. Rev. Mol. Cell Biol.* **6**, 622-634.

Haag, J. and Aigner, T. (2007). Identification of calponin 3 as a novel Smad-binding modulator of BMP signaling expressed in cartilage. *Exp. Cell Res.* **313**, 3386-3394.

Harada, N., Tamai, Y., Ishikawa, T., Sauer, B., Takaku, K., Oshima, M. and Taketo, M. M. (1999). Intestinal polyposis in mice with a dominant stable mutation of the beta-catenin gene. *EMBO J.* **18**, 5931-5942.

Haramis, A. P., Begthel, H., van den Born, M., van Es, J., Jonkheer, S., Offerhaus, G. J. and Clevers, H. (2004). De novo crypt formation and juvenile polyposis on BMP inhibition in mouse intestine. *Science* **303**, 1684-1686.

Hazan, R. B., Qiao, R., Keren, R., Badano, I. and Suyama, K. (2004). Cadherin switch in tumor progression. *Ann. NY Acad. Sci.* **1014**, 155-163.

He, X. C., Zhang, J., Tong, W. G., Tawfik, O., Ross, J., Scoville, D. H., Tian, Q., Zeng, X., He, X., Wiedemann, L. M. et al. (2004). BMP signaling inhibits intestinal stem cell self-renewal through suppression of Wnt-beta-catenin signaling. *Nat. Genet.* **36**, 1117-1121.

Hermiston, M. L. and Gordon, J. I. (1995). In vivo analysis of cadherin function in the mouse intestinal epithelium: essential roles in adhesion, maintenance of differentiation, and regulation of programmed cell death. *J. Cell Biol.* **129**, 489-506.

Hermiston, M. L., Wong, M. H. and Gordon, J. I. (1996). Forced expression of E-cadherin in the mouse intestinal epithelium slows cell migration and provides evidence for nonautonomous regulation of cell fate in a self-renewing system. *Genes Dev.* **10**, 985-996.

Kan, N. G., Stemmler, M. P., Junghans, D., Kanzler, B., de Vries, W. N., Dominis, M. and Kemler, R. (2007). Gene replacement reveals a specific role for E-cadherin in the formation of a functional trophectoderm. *Development* **134**, 31-41.

Kemler, R. (1993). From cadherins to catenins: cytoplasmic protein interactions and regulation of cell adhesion. *Trends Genet.* **9**, 317-321.

Kim, K. A., Kakitani, M., Zhao, J., Oshima, T., Tang, T., Binnerts, M., Liu, Y., Boyle, B., Park, E., Emtage, P. et al. (2005). Mitogenic influence of human R-spondin1 on the intestinal epithelium. *Science* **309**, 1256-1259.

Kim, K. A., Wagle, M., Tran, K., Zhan, X., Dixon, M. A., Liu, S., Gros, D., Korver, W., Yonkovich, S., Tomasevic, N. et al. (2008). R-Spondin family members regulate the Wnt pathway by a common mechanism. *Mol. Biol. Cell* **19**, 2588-2596.

Klapholz-Brown, Z., Walmsley, G. G., Nusse, Y. M., Nusse, R. and Brown, P. O. (2007). Transcriptional program induced by Wnt protein in human fibroblasts suggests mechanisms for cell cooperativity in defining tissue microenvironments. *PLoS ONE* **2**, e945.

Lin, Z., Gao, C., Ning, Y., He, X., Wu, W. and Chen, Y. G. (2008). The pseudoreceptor BMP and activin membrane-bound inhibitor positively modulates Wnt/beta-catenin signaling. *J. Biol. Chem.* **283**, 33053-33058.

Liu, Y., Li, Q. C., Miao, Y., Xu, H. T., Dai, S. D., Wei, Q., Dong, Q. Z., Dong, X. J., Zhao, Y., Zhao, C. et al. (2009). Ablation of p120-catenin enhances invasion and metastasis of human lung cancer cells. *Cancer Sci.* **100**, 441-448.

Mermelshtein, A., Gerson, A., Walfisch, S., Delgado, B., Shechter-Maor, G., Delgado, J., Fich, A. and Gheber, L. (2005). Expression of D-type cyclins in colon cancer and in cell lines from colon carcinomas. *Br. J. Cancer* **93**, 338-345.

Orsulic, S., Huber, O., Aberle, H., Arnold, S. and Kemler, R. (1999). E-cadherin binding prevents beta-catenin nuclear localization and beta-catenin/LEF-1-mediated transactivation. *J. Cell Sci.* **112**, 1237-1245.

Oshima, M., Oshima, H., Kitagawa, K., Kobayashi, M., Itakura, C. and Taketo, M. (1995). Loss of Apc heterozygosity and abnormal tissue building in nascent intestinal polyps in mice carrying a truncated Apc gene. *Proc. Natl. Acad. Sci. USA* **92**, 4482-4486.

Pinto, D. and Clevers, H. (2005). Wnt, stem cells and cancer in the intestine. *Biol. Cell* **97**, 185-196.

Pinto, D., Gregorieff, A., Begthel, H. and Clevers, H. (2003). Canonical Wnt signals are essential for homeostasis of the intestinal epithelium. *Genes Dev.* **17**, 1709-1713.

Scott, J. A. and Yap, A. S. (2006). Cinderella no longer: alpha-catenin steps out of cadherin's shadow. *J. Cell Sci.* **119**, 4599-4605.

Seidel, B., Braeg, S., Adler, G., Wedlich, D. and Menke, A. (2004). E- and N-cadherin differ with respect to their associated p120ctn isoforms and their ability to suppress invasive growth in pancreatic cancer cells. *Oncogene* **23**, 5532-5542.

Sekiya, T., Adachi, S., Kohu, K., Yamada, T., Higuchi, O., Furukawa, Y., Nakamura, Y., Nakamura, T., Tashiro, K., Kuhara, S. et al. (2004). Identification of BMP and activin membrane-bound inhibitor (BAMBI), an inhibitor of transforming growth factor-beta signaling, as a target of the beta-catenin pathway in colorectal tumor cells. *J. Biol. Chem.* **279**, 6840-6846.

Stemmler, M. P. (2008). Cadherins in development and cancer. *Mol. Biosyst.* **4**, 835-850.

Su, L. K., Kinzler, K. W., Vogelstein, B., Preisinger, A. C., Moser, A. R., Luongo, C., Gould, K. A. and Dove, W. F. (1992). Multiple intestinal neoplasia caused by a mutation in the murine homolog of the APC gene. *Science* **256**, 668-670.

Suyama, K., Shapiro, I., Guttman, M. and Hazan, R. B. (2002). A signaling pathway leading to metastasis is controlled by N-cadherin and the FGF receptor. *Cancer Cell* **2**, 301-314.

Takeichi, M. (1988). The cadherins: cell-cell adhesion molecules controlling animal morphogenesis. *Development* **102**, 639-655.

Takeichi, M. (2007). The cadherin superfamily in neuronal connections and interactions. *Nat. Rev. Neurosci.* **8**, 11-20.

Tetsu, O. and McCormick, F. (1999). Beta-catenin regulates expression of cyclin D1 in colon carcinoma cells. *Nature* **398**, 422-426.

Tian, Q., Feetham, M. C., Tao, W. A., He, X. C., Li, L., Aebersold, R. and Hood, L. (2004). Proteomic analysis identifies that 14-3-3zeta interacts with beta-catenin and facilitates its activation by Akt. *Proc. Natl. Acad. Sci. USA* **101**, 15370-15375.

Tian, Q., He, X. C., Hood, L. and Li, L. (2005). Bridging the BMP and Wnt pathways by PI3 kinase/Akt and 14-3-3zeta. *Cell Cycle* **4**, 215-216.

Tomita, K., van Bokhoven, A., van Leenders, G. J., Ruijter, E. T., Jansen, C. F., Bussemakers, M. J. and Schalken, J. A. (2000). Cadherin switching in human prostate cancer progression. *Cancer Res.* **60**, 3650-3654.

Traber, P. G., Gumucio, D. L. and Wang, W. (1991). Isolation of intestinal epithelial cells for the study of differential gene expression along the crypt-villus axis. *Am. J. Physiol.* **260**, G895-G903.

van de Wetering, M., Sancho, E., Verweij, C., de Lau, W., Oving, I., Hurlstone, A., van der Horn, K., Batlle, E., Coudreuse, D., Haramis, A. P. et al. (2002). The beta-catenin/TCF-4 complex imposes a crypt progenitor phenotype on colorectal cancer cells. *Cell* **111**, 241-250.

van der Flier, L. G., van Gijn, M. E., Hatzis, P., Kujala, P., Haegebarth, A., Stange, D. E., Begthel, H., van den Born, M., Guryev, V., Oving, I. et al. (2009). Transcription factor achaete scute-like 2 controls intestinal stem cell fate. *Cell* **136**, 903-912.

van Noort, M., Meeldijk, J., van der Zee, R., Destree, O. and Clevers, H. (2002). Wnt signaling controls the phosphorylation status of beta-catenin. *J. Biol. Chem.* **277**, 17901-17905.

Waite, K. A. and Eng, C. (2003). From developmental disorder to heritable cancer: it's all in the BMP/TGF-beta family. *Nat. Rev. Genet.* **4**, 763-773.

Wheelock, M. J., Shintani, Y., Maeda, M., Fukumoto, Y. and Johnson, K. R. (2008). Cadherin switching. *J. Cell Sci.* **121**, 727-735.

Wildenberg, G. A., Dohn, M. R., Carnahan, R. H., Davis, M. A., Lobdell, N. A., Settleman, J. and Reynolds, A. B. (2006). p120-catenin and p190RhoGAP regulate cell-cell adhesion by coordinating antagonism between Rac and Rho. *Cell* **127**, 1027-1039.

Yilmaz, M. and Christofori, G. (2009). EMT, the cytoskeleton, and cancer cell invasion. *Cancer Metastasis Rev.* **28**, 15-33.

Zeilstra, J., Joosten, S. P., Dokter, M., Verwiel, E., Spaargaren, M. and Pals, S. T. (2008). Deletion of the WNT target and cancer stem cell marker CD44 in Apc(Min/+) mice attenuates intestinal tumorigenesis. *Cancer Res.* **68**, 3655-3661.